Magnon-Induced Nonreciprocity in a Non-Hermitian Cavity Magnonic System

Mei Wang, Gui-Ling Xiao, Duo Zhang, Deng Wei Zhang, Zhao-Yu Sun, and Li-Li Zheng

***Abstract*— Microwave nonreciprocity is in high demand for applications in information processing. Here, we propose an effective approach to realize robust microwave transmission nonreciprocity in a three-mode non-Hermitian cavity magnetic system (CMS). We show that, around the exceptional point, robust microwave nonreciprocity can be achieved within a small detuning range between the cavity and the microwave field. It is fundamentally induced by means of the cavity-magnon interaction and the effective magnon Kerr nonlinearity. Moreover, in the vicinity of the exceptional point, robust microwave transmission nonreciprocity can be realized over an optimal magnetic field range. This greatly improves the operability for obtaining strong microwave nonreciprocity experimentally. This study may stimulate further investigations and applications of the non-Hermitian CMS in structuring high-performance nonreciprocal devices.**

***Index Terms*—Microwave nonreciprocity, non-Hermitian, cavity magnonic system.**

I. Introduction

OWING to the potential and great application prospects of quantum technology, many quantum manipulation platforms have received extensive international attention, such as optomechanical system [1], [2], [3], [4], cavity quantum electrodynamical systems [5], [6] and so on. Specially, cavity magnonics systems [7], [8], [9], [10], [11], [12], [13], [14], [15], [16], [17] have become a new research hotspot in recent years. It is generally composed of a microwave cavity and magnons, i.e., the massive collective spin excitations in ferroand ferrimagnetic materials such as yttrium iron garnet (YIG), where magnons are strongly coupled to microwave photons. Benefitting from the advantages of low dissipation and high extensibility, compound information interaction platforms can be structured via establishing the interaction of magnon to (artificial) atoms [18], acoustic phonons [19], [20], [21], [22], optical photons [23], [24], or superconducting coplanar microwave resonator [25]. Furthermore, due to the long coherence time as well as intrinsically high tunability, a series of novel and interesting phenomena have been studied. One of the most notable is nonreciprocity [26], [27], [28], [29], which, associated with the breaking of Lorentz reciprocity, is manifested as propagation of signal in one direction but not the other. Nonreciprocity physics provides the core technologies for communication and information processing, such as implementing one-way signal communication and manufacturing chip-scale nonreciprocal devices: isolator, metamaterials and circulator.

On the other hand, the latest developments in two-mode non-Hermitian physics [30] provide a bounty of opportunities for a broad range of basic research and engineering applications. This is owing to the unique characteristic of two-mode non-Hermitian systems, e.g., the exceptional point [31], [32], where both eigenvalues and their corresponding eigenvectors simultaneously coalesce. Based on such exceptional point, a large number of theoretical and experimental studies have been carried out successfully from the fields of quantum mechanics [33], [34], optics [35], [36], [37], [38], [39], [40], [41], microwaves [42], [43], electronics [44], [45], mechanics [46], [47], [48], and thermology [49]. Such as experimental observation of the topological structure of exceptional points [50], optical non-reciprocity [51], [52], loss-induced transparency [37], low power optical diodes [53], [54], a single-mode laser [55], [56], PT-symmetric phonon laser [52], PT-symmetry-enhanced optical high-order sideband generation [57], PT-symmetry-breaking induced ultra-low threshold chaos [58], PT-symmetry-breaking-enhanced cavity optomechanical magnetometry [59], PT-symmetric magnon laser in cavity optomagnonics [60] and so on. Most of these studies are performed in a two-mode non-Hermitian system. A question arises spontaneously whether there is an exceptional point in a strongly coupled three-mode non-Hermitian system. If it exists, could it affect the transmission nonreciprocity of the three-mode non-Hermitian system?

Inspired by the experiment in a standard CMS where the higher-order exceptional point are studied [61], in this work, we propose a scheme to explore microwave transmission nonreciprocity in a three-mode non-Hermitian CMS. This compound CMS is composed of a couple of gain-loss microwave cavities and one dissipative YIG sphere. In contrast to the two-mode non-Hermitian system composed of two gain-loss microwave cavities, the three-mode non-Hermitian CMS features a shifted exceptional point marked by the microwave photon-tunneling

Manuscript received 14 September 2023; revised 17 October 2023; accepted 25 October 2023. Date of publication 30 October 2023; date of current version 7 December 2023. This work was supported in part by the National Natural Science Foundation of China (NSFC) under Grants 12105210, 12005078, and 12304395, and in part by the Knowledge Innovation Program of Wuhan-Basi Research under Grant 2023010201010149. *(Corresponding authors: Mei Wang; Li-Li Zheng.)*

Mei Wang, Gui-Ling Xiao, Duo Zhang, and Zhao-Yu Sun are with the School of Electrical Engineering, Wuhan Polytechnic University, Wuhan 430040, China (e-mail: wangmei_2@vip163.com).

Deng Wei Zhang is with the Department of Mathematics and Physics, Luoyang Institute of Science and Technology, Luoyang 471026, China.

Li-Li Zheng is with the Key Laboratory of Optoelectronic Chemical Materials and Devices of Ministry of Education, Jianghan University, Wuhan 430074, China (e-mail: zhenglili@jhun.edu.cn).

Digital Object Identifier 10.1109/JPHOT.2023.3328381

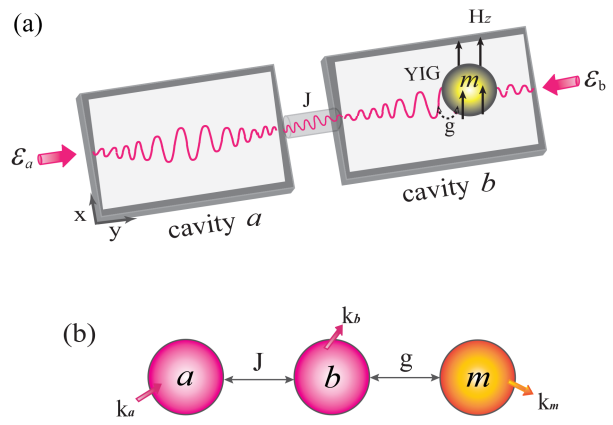

Fig. 1. (Color online) (a) Schematic diagram of a three-mode non-hermitian CMS consisting of two coupled three-dimensional rectangular microwave cavities and a YIG sphere. (b) In this three-mode non-Hermitian CMS, the passive cavity b (with decay rate κ_b) is linearly coupled to an active cavity a (with gain rate κ_a) and the magnon mode m in YIG sphere (with decay rate κ_m), the cavity-cavity coupling strength is J and the cavity-magnon interaction strength is g.

rate when other parameters are fixed. We find, in the vicinity of the exceptional point, huge asymmetry of the microwave transmissions in two directions can be obtained. Physically, this is induced by the cavity-magnon interaction and the effective magnon Kerr nonlinearity in the system. Consequently, robust microwave transmission nonreciprocity marked by the high isolation ratio can be generated. More importantly, near the exceptional point, strong microwave transmission nonreciprocity can be captured over an optimal magnetic field range, which tunes the frequency of the magon mode. This finding greatly improves the feasibility of experiment. It may stimulate further investigations and applications of the three-mode non-Hermitian CMS in information processing.

This article is organized as follows: In Section II, we introduce the theoretical scheme of the three-mode non-hermitian CMS and its effective Hamiltonian with the external driving fields. Then we derive the transmission coefficients of the microwave field in two cases and the corresponding nonreciprocity isolation ratio. In Section III, we theoretically analyze the regulation of the magnon mode on the microwave transmission nonreciprocity under different microwave photon-tunneling rates in the three-mode non-hermitian CMS. Conclusions are finally given in Section IV.

II. The Model and the Formulas Derivation

As schematically shown in Fig. 1(a) and (b), we consider a three-mode non-Hermitian CMS, which consists of an active three-dimensional rectangular microwave cavity and a passive three-dimensional rectangular microwave cavity [63] where a lossy YIG sphere is located. Including the driving part, the Hamiltonian of the whole system is given as

$$\hat{H} = \hat{H}_s + \hat{H}_d, \tag{1}$$

where

$$\hat{H}_s/\hbar = \Delta_c(\hat{a}^\dagger\hat{a} + \hat{b}^\dagger\hat{b}) + \Delta_m\hat{m}^\dagger\hat{m} + J(\hat{a}^\dagger\hat{b} + \hat{a}\hat{b}^\dagger) + K\hat{m}^\dagger\hat{m}\hat{m}^\dagger\hat{m} + g(\hat{b}^\dagger\hat{m} + \hat{b}\hat{m}^\dagger),$$
$$\hat{H}_d/\hbar = i\sqrt{\eta_a\kappa_a}\varepsilon_a(\hat{a}^\dagger - \hat{a}) + i\sqrt{\eta_b\kappa_b}\varepsilon_b(\hat{b}^\dagger - \hat{b}),$$

here, $\hat{a}$ ($\hat{a}^\dagger$), $\hat{b}$ ($\hat{b}^\dagger$) and $\hat{m}$ ($\hat{m}^\dagger$) are the annihilation (creation) operators of the active cavity mode, the passive cavity mode and the magnon mode, respectively. The active cavity $\hat{a}$ (with frequency ω_c) resonantly couples to the passive cavity $\hat{b}$ where a YIG sphere is located, with coupling strength J. For the the magnon mode $\hat{m}$, i.e., representing the massive collective spin excitation in the YIG sphere, couples to the microwave cavity $\hat{b}$ with coupling strength g. Frequency of the magnon is determined by the uniformly DC bias magnetic field H_z as shown in Fig. 1(a). The Kerr nonlinear coefficient $K = \mu_0 K_{an}\gamma^2/(M^2V_m)$, originating from the magnetocrystalline anisotropy in the YIG sphere, where μ_0 is the magnetic permeability of free space, K_{an} is the first-order anisotropy constant, γ is the gyromagnetic ratio, M is the saturation magnetization, and V_m is the volume of the YIG sphere. In addition, each of the cavities, is, respectively, driven by a monochromatic microwave field with amplitude ε_a and ε_b at frequency ω_d. Here ε_a (ε_b) is related to the input power P_a (P_b) and the gain rate κ_a (the dissipation rate κ_b) by $\varepsilon_a = \sqrt{P_a/\hbar\omega_d}$ ($\varepsilon_b = \sqrt{P_b/\hbar\omega_d}$). The frequency detunings $\Delta_c = \omega_c - \omega_d$ and $\Delta_m = \omega_m - \omega_d$. κ_j ($j = a, b, m$) represents the total gain or dissipation of any microwave cavity or magnon with the coupling parameter η_j.

As a non-Hermitian system (see Fig. 1(b)), whose non-Hermitian Hamiltonian can be written as

$$\hat{H}_n/\hbar = \hat{H}_s/\hbar + i\frac{\kappa_a}{2}\hat{a}^\dagger\hat{a} - i\frac{\kappa_b}{2}\hat{b}^\dagger\hat{b} - i\frac{\kappa_m}{2}\hat{m}^\dagger\hat{m}. \tag{2}$$

Based on the Hamiltonian, we find the current CMS exhibits a critical point marked by the cavity-cavity coupling strength J/κ_b. This point is similar to that of the two-mode non-Hermitian system [61], [62]. As shown in Fig. 2(a), when the cavity-magnon coupling disappears, namely, $g/\kappa_b = 0$, the system is simplified as a two-mode non-Hermitian system and the system exceptional point is $J/\kappa_b = 0.4$ (corresponding to green-dotted line), where the system eigenvalues and their corresponding eigenvectors of the system simultaneously coalesce. Once the cavity-magnon coupling rate g/κ_b is enhanced to 0.2 in Fig. 2(b), the system exceptional point is shifted to $J/\kappa_b = 0.4386$. Here, it is worth noting that the system eigenvalues $(\omega_{1/2/3} - \omega_c)$ and their corresponding eigenvectors may not simultaneously coalesce at the exceptional point. It can be seen that the system eigenvalues stay relatively constant, when the coupling strength J/κ_b is smaller than 0.4386. However, once this critical point is passed, the eigenvalues immediately vary with the value of J/κ_b. In addition, the magnon dissipation also has a direct impact on the system eigenvalues. As shown in Fig. 2(b), (c) and (d), the exceptional points change with the successive increase of the magnon dissipations. Furthermore, we find that the distribution of the system eigenvalues tends to a two-mode system when the magnon dissipation is strong enough (refer to Fig. 2(d)). This shows that the existence of the

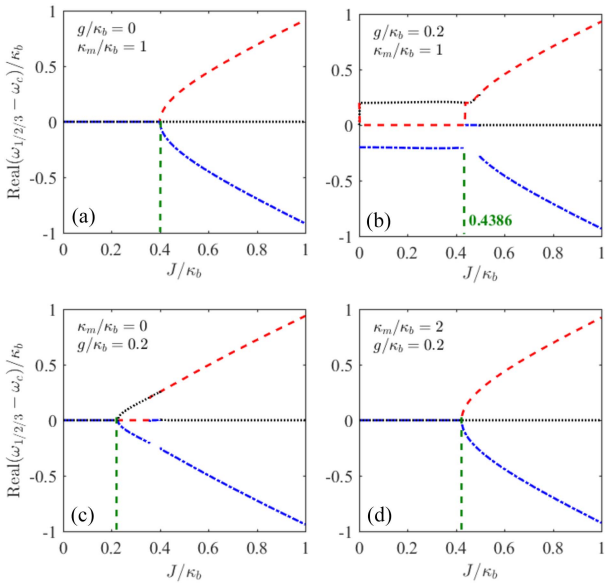

Fig. 2. (Color online) The real parts of the eigenvalues $(\omega_{1/2/3} - \omega_c)/\kappa_b$ of the three-mode non-Hermitian system vs the microwave photon-tunneling strength J/κ_b. The microwave cavity-magnon coupling strengths $g/\kappa_b = 0, \tilde{}0.2$ in panels (a) and (b), respectively, with $\kappa_m/\kappa_b = 1$. The dissipative rates of the magnon $\kappa_m/\kappa_b = 0, \tilde{}2$ in (c) and (d), respectively, with $g/\kappa_b = 0.2$. Other parameters are given as $\kappa_b = 10\,\mathrm{MHz}$, $\kappa_a/\kappa_b = 0.6$, $\eta_a = \eta_b = \eta_m = \frac{1}{2}$, $\omega_c/2\pi = \omega_m/2\pi = 10.1\,\mathrm{GHz}$, $\Delta_c = \Delta_m = 0$, $K/2\pi = 3.8 \times 10^{-9}\,\mathrm{Hz}$, $P_a = P_b = 1\,\mu\mathrm{W}$.

magnon in the system may significantly affect the system dynamic behavior. So in the following content, we keep $g/\kappa_b = 0.2$ and $\kappa_m/\kappa_b = 1$ to ensure the exceptional point $J/\kappa_b = 0.4386$. The other parameters are set based on relevant experiments [61], [63].

To study the system dynamic evolution, we employ the Heisenberg-Langevin equations by setting $< \hat{o} >= o$ ($\hat{o}$ is a normal annihilation operator) in the semiclassical limit, namely,

$$\dot{a} = (-i\Delta_c + \frac{\kappa_a}{2})a - iJb + \sqrt{\eta_a\kappa_a}\varepsilon_a, \tag{3}$$

$$\dot{b} = (-i\Delta_c - \frac{\kappa_b}{2})b - iJa - igm + \sqrt{\eta_b\kappa_b}\varepsilon_b, \tag{4}$$

$$\dot{m} = (-i\Delta_m - \frac{\kappa_m}{2})m - igb - iK(2|m|^2 + 1)m, \tag{5}$$

here, (3), (4) and (5) respectively describes the dynamic evolution of cavities a, b and the magnon mode m. To solve above Equations, we divide operators of the microwave photons and the magnon into two parts, the steady-state mean values and the perturbations, i.e., $a = \mathrm{A_s} + \delta a$, $b = \mathrm{B_s} + \delta b$ and $m = \mathrm{M_s} + \delta m$. Taking these deformation into above equations and combining the condition $d\mathrm{A_s}/dt = 0$, $d\mathrm{B_s}/dt = 0$ and $d\mathrm{M_s}/dt = 0$, the steady-state differential equations can be derived as

$$0 = (-i\Delta_c + \frac{\kappa_a}{2})\mathrm{A_s} - iJ\mathrm{B_s} + \sqrt{\eta_a\kappa_a}\varepsilon_a, \tag{6}$$

$$0 = (-i\Delta_c - \frac{\kappa_b}{2})\mathrm{B_s} - iJ\mathrm{A_s} - ig\mathrm{M_s} + \sqrt{\eta_b\kappa_b}\varepsilon_b, \tag{7}$$

$$0 = (-i\Delta_m - \frac{\kappa_m}{2})\mathrm{M_s} - ig\mathrm{B_s} - iK(2|\mathrm{M_s}|^2 + 1)\mathrm{M_s}. \tag{8}$$

To make it easier to distinguish, when the driving field is injected upon cavity a, the steady-state mean values $\mathrm{A_s}$, $\mathrm{B_s}$ and $\mathrm{M_s}$ are deformed from (6), (7) and (8) as

$$\mathrm{A_{sa}} = \frac{\sqrt{\eta_a\kappa_a}\varepsilon_a - iJ\mathrm{B_{sa}}}{i\Delta_c - \frac{\kappa_a}{2}}, \tag{9}$$

$$\mathrm{B_{sa}} = \frac{g(\Delta_c + i\frac{\kappa_a}{2})\mathrm{M_{sa}} - iJ\sqrt{\eta_a\kappa_a}\varepsilon_a}{(i\Delta_c - \frac{\kappa_a}{2})(i\Delta_c + \frac{\kappa_b}{2}) + J^2}, \tag{10}$$

$$\mathrm{M_{sa}} = \frac{-gJ\sqrt{\eta_a\kappa_a}\varepsilon_a}{\left[(i\Delta_c - \frac{\kappa_a}{2})(i\Delta_c + \frac{\kappa_b}{2}) + J^2\right]\Theta}, \tag{11}$$

in which

$$\Theta = i(\Delta_m + 2K|\mathrm{M_{sa}}|^2 + K) + \frac{\kappa_m}{2} + \frac{g^2(i\Delta_c - \frac{\kappa_a}{2})}{(i\Delta_c - \frac{\kappa_a}{2})(i\Delta_c + \frac{\kappa_b}{2}) + J^2}. \tag{12}$$

With the input-output relation, the output field of the microwave from cavity b can be expressed as

$$S_{aout} = \sqrt{\eta_b\kappa_b}\mathrm{B_{sa}}. \tag{13}$$

In the direction from cavity a to b, the microwave transmission coefficient is given as

$$\mathrm{T_a} = \left|\frac{\sqrt{\eta_b\kappa_b}\mathrm{B_{sa}}}{\varepsilon_a}\right|. \tag{14}$$

When the driving field acting only on cavity b, the steady-state mean values can be given as

$$\mathrm{A_{sb}} = \frac{-iJ\mathrm{B_{sb}}}{i\Delta_c - \frac{\kappa_a}{2}}, \tag{15}$$

$$\mathrm{B_{sb}} = \frac{g(\Delta_c + i\frac{\kappa_a}{2})\mathrm{M_{sb}} + (i\Delta_c - \frac{\kappa_a}{2})\sqrt{\eta_b\kappa_b}\varepsilon_b}{(i\Delta_c - \frac{\kappa_a}{2})(i\Delta_c + \frac{\kappa_b}{2}) + J^2}, \tag{16}$$

$$\mathrm{M_{sb}} = \frac{gJ(\Delta_c + i\frac{\kappa_a}{2})\sqrt{\eta_b\kappa_b}\varepsilon_b}{\left[(i\Delta_c - \frac{\kappa_a}{2})(i\Delta_c + \frac{\kappa_b}{2}) + J^2\right]\vartheta}. \tag{17}$$

where

$$\vartheta = i(\Delta_m + 2K|\mathrm{M_{sb}}|^2 + K) + \frac{\kappa_m}{2} + \frac{g^2(i\Delta_c - \frac{\kappa_a}{2})}{(i\Delta_c - \frac{\kappa_a}{2})(i\Delta_c + \frac{\kappa_b}{2}) + J^2}. \tag{18}$$

Similarly, in this case the output field of the microwave field from cavity a can be expressed as follows:

$$S_{bout} = \sqrt{\eta_a\kappa_a}\mathrm{A_{sb}}. \tag{19}$$

The transmission coefficient of the microwave field from cavity b to cavity a is given as

$$\mathrm{T_b} = \left|\frac{\sqrt{\eta_a\kappa_a}\mathrm{A_{sb}}}{\varepsilon_b}\right|. \tag{20}$$

In order to more intuitively and clearly describe the nonreciprocal transmission of the microwave fields along two directions, we introduce definition of the nonreciprocal isolation ratio,

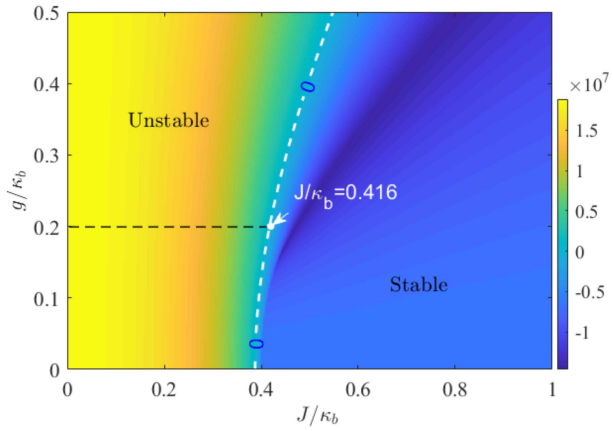

Fig. 3. (Color online) Parameter regime of the stability in the three-mode non-Hermitian cavity magnetic system with different microwave photon-tunneling rates J/κ_b and cavity-magnon coupling strength g/κ_b when the driving power $P_a(P_b) = 1\mu$W. Here we set $\kappa_m/\kappa_b = 1$ and the other parameters are same as that in Fig. 2.

which is expressed as

$$I = 10\left|\log_{10}\frac{|\sqrt{\eta_b\kappa_b}\mathrm{B_{sa}}|^2}{|\sqrt{\eta_a\kappa_a}\mathrm{A_{sb}}|^2}\right|, \tag{21}$$

which can quantitatively describe the degree of nonreciprocity of the microwave transmissions between two directions. Specifically, when $I = 0$, equivalently, $\frac{|\sqrt{\eta_b\kappa_b}\mathrm{B_{sa}}|^2}{|\sqrt{\eta_a\kappa_a}\mathrm{A_{sb}}|^2} = 1$, it means that microwave transmissions along two opposite directions are reciprocal. For other cases, the larger the value of I, the higher the degree of nonreciprocity of the microwave transmissions along two directions. For instance, when $I \geq 1$, it states that the transmittance in one direction is at least 10 times higher than the other. If the value of I is large enough, one-way transmission of the microwave field may occur.

From the point of another angle, the system gain and the Kerr nonlinearity processes can also induce instability. In Fig. 3 we show the numerical stability condition for the system with the driving power $P_a(P_b) = 1\mu$W. In the following content, the cavity-magnon coupling strength $g/\kappa_b = 0.2$ is choosed and the microwave photon-tunneling rates J/κ_b are used in the stable regime.

III. Magnon-Induced Nonreciprocity of the Microwave Field in a Non-Hermitian Cavity Magnonical System

Through above theoretical derivation, it can be seen that the transmission coefficients in (14) and (20) are closely dependent on the microwave photon-tunneling rate J. When J is in different regions, i.e., being smaller or larger than the exceptional point 0.4386, may lead to entirely different system transmission properties. Then we analyze the transmission properties of the system under different microwave photon-tunneling rates.

A. Dependence of the Nonreciprocal Transmission on the Microwave Photon-Tunneling Rate J

As a precondition, the frequency detunings are chosen as $\Delta_c = \Delta_m = \Delta$, namely, the microwave cavities and the

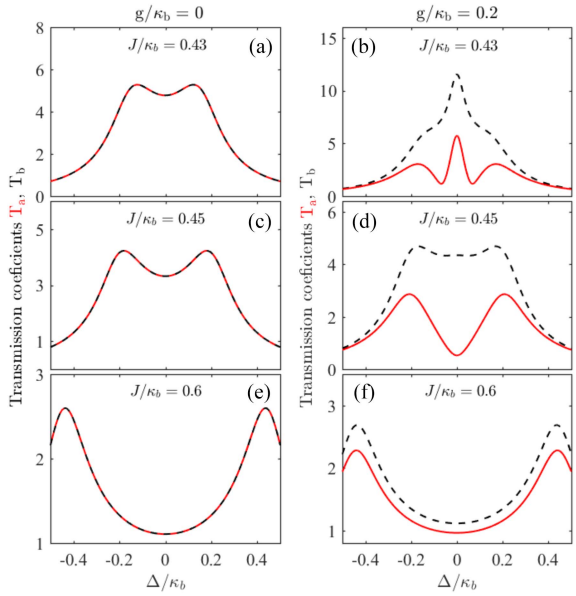

Fig. 4. (Color online) Transmission coefficients T_a and T_b of the microwave field vs frequency detuning Δ/κ_b with different microwave photon-tunneling rates J/κ_b, in the cases of the cavity-magnon coupling strengths $g/\kappa_b = 0$ and 0.2, respectively. Here $J/\kappa_b = 0.43$ in (a) and (b), $J/\kappa_b = 0.45$ in (c) and (d), $J/\kappa_b = 0.6$ in (e) and (f). Here $\Delta_c = \Delta_m = \Delta$ and $\kappa_m/\kappa_b = 1$, other parameters are given as those in Fig. 2.

magnon mode are resonantly coupled. In order to analyze the transmission nonreciprocity in a three-mode non-Hermitian system more thoroughly, we first set $g/\kappa_b = 0$ to simplify the system into a two-coupled microwave cavities with the exceptional point $J/\kappa_b = 0.4$. As shown in Fig. 4(a), (c), and (e), the transmission coefficients T_a and T_b, varying with frequency detuning Δ/κ_b between the driving field and the cavity under different values of J/κ_b, are schematically plotted. We can intuitively see the transmission coefficients T_a and T_b are completely reciprocal with the increase of J/κ_b. Then tunning the cavity-magnon interaction strength $g/\kappa_b = 0.2$, we focus on the transmission coefficients in a three-mode non-Hermitian CMS with exceptional point $J/\kappa_b = 0.4386$. By regulating the microwave photon-tunneling rate J/κ_b, we first let the system enter into the region $J/\kappa_b < 0.4386$. It can be seen from Fig. 4(b) that transmission coefficient T_b reaches its peak value 12 at $\Delta/\kappa_b = 0$. While T_a shows three peaks, in which the center peak reaches 6 at $\Delta/\kappa_b = 0$ and the other two lower peaks are symmetrically distributed about this point. The transmission coefficients exhibit significantly strong nonreciprocity in the near resonant region. Then we increase J/κ_b to 0.45 beyond the exceptional point. As shown in Fig. 4(d), transmission coefficients T_a and T_b each have two peaks which are symmetrically distributed with respect to $\Delta/\kappa_b = 0$. What's more, there is a large gap between the transmission coefficients T_a and T_b. Continue to increase J/κ_b to 0.6 in Fig. 4(f), two symmetric sideband peaks of T_a and T_b shift towards both sides compared to Fig. 4(d). In the meantime, the gap between them gradually decreases as the coupling strength J/κ_b moves away from the exceptional point. These results imply that, in the three-mode non-Hermitian system, the microwave transmissions along two directions have

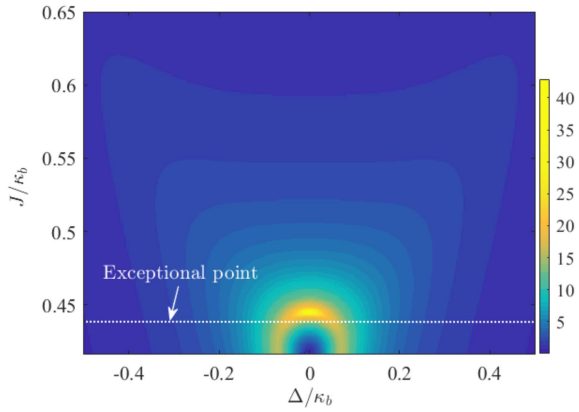

Fig. 5. (Color online) The isolation ratio I vs the microwave photon-tunneling rate J/κ_b and frequency detuning Δ/κ_b. Other parameters are the same as described in the caption of Fig. 2.

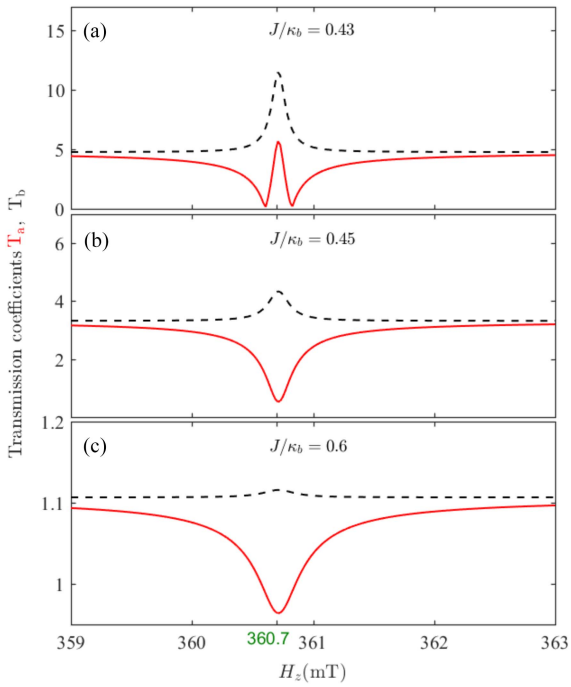

Fig. 6. (Color online) Transmission coefficients T_a and T_b of the microwave fields vs the uniformly DC magnetic bias field strength H_z with different microwave photon-tunneling rates J/κ_b in the non-Hermitian CMS. Here $J/\kappa_b = 0.43,\ 0.45,\ 0.6$ in (a), (b) and (c), respectively. The frequency detuning $\Delta_c = 0$, other parameters are same as those in Fig. 2.

strong nonreciprocity near the exception point. Compared to the case $g/\kappa_b = 0$, it is not difficult to find that the emergence of the strong microwave transmission nonreciprocity is mainly stimulated by the magnon mode in the system. Essentially, it benefits from the combined effect of the cavity-magnon resonant interaction and the effective magnon Kerr nonlinearity, specially, near the exceptional point. Further more, we find an interesting phenomenon from Fig. 4. The transmission coefficient along cavities b to a is always higher than that in the opposite direction. So this device can be used to structure microwave isolators under appropriate parameters of J and detuning Δ.

In order to quantitatively describe the nonreciprocity of microwave transmission, the nonreciprocal isolation ratio I as a function of J and the frequency detuning Δ is rendered in Fig. 5. Here, the microwave photon-tunneling rate is in the stable range $J/\kappa_b \in [0.416 \quad 0.65]$ with other parameters fixed (as in Fig. 5). We can see the high isolation ratios are mainly concentrated in the bright area shaped as a crescent moon, which has a symcenter of $\Delta/\kappa_b = 0$. It is worth noting that the bright area only appears near the exceptional point (corresponding to the white dotted line) in the optimal detuning range $\Delta/\kappa_b \in [0.3 \quad 0.3]$. The isolation ratio decreases rapidly when J/κ_b is far away from the exceptional point. These results are consistent with the evolution processes of the transmission coefficients in Fig. 4(b), (d) and (f). It implies that, near the exceptional point, the robust transmission nonreciprocity of the microwave field can be induced in a three-mode non-Hermitian CMS within the optimal detuning, based on the joint effect of the cavity-magnon resonant interaction and the effective magnon Kerr nonlinearity. This may offer a new method to build microwave amplifiers [64], [65] and isolators [66], [67].

B. Dependence of the Nonreciprocal Transmission on the DC Bias Magnetic Field H_z Acting on the YIG Sphere

In the previous subsection, the cavity and magnon are resonant coupled, i.e., $\Delta_c = \Delta_m$. In what follows, we explore the influence of the frequency detunning between the cavity and the mangon on the transmission nonreciprocity in the system under different microwave photon-tunneling rates. Physically, the magnon's frequency is tuned by the external uniformly DC magnetic field H_z applied on the YIG sphere. Therefore, it directly determines the frequency detunning between the cavity and the magnon modes when other system parameters keep constant.

Fig. 6 shows the transmission coefficients vary with the external magnetic field with different microwave photon-tunneling rates. We set $J/\kappa_b = 0.43$ near the exceptional point in Fig. 6(a). The curve of T_a shows a peak at $H_z = 360.7$mT (where the magnon and the microwave cavity are resonantly coupled) and two symmetrically distributed dips around it. While T_b exhibits a sharp peak at $H_z = 360.7$mT. It can be seen that T_a and T_b have significant asymmetry, within the small detuning range, which represents strong transmission nonreciprocity. Then, crossing the exceptional point, we use $J/\kappa_b = 0.45$ in Fig. 6(b) and 0.6 in Fig. 6(c), respectively. The evolution trajectories of T_a and T_b are highly similar in both panels. The evolutions of both T_b remain stable, except for the shallow peaks at the resonance point; both of T_a keep stable until the relatively wide valleys appear near the resonance point. Carefully comparing the transmission coefficients in the two panels, we find that the transmission coefficients T_a and T_b, as well as the gap between them, gradually decrease as J increases. This result implies that strong microwave transmission nonreciprocity along two directions can be realized near the resonant point $H_z = 360.7$ mT, as long as J/κ_b is appropriately given around the exceptional point. The fact is due to the more easy enhancement of

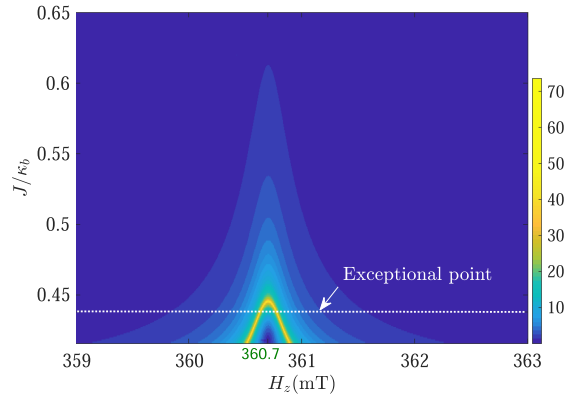

Fig. 7. (Color online) The isolation ratio I vs the cavity-cavity coupling strength J and the magnetic field H_z. The other parameters are the same as described in the caption of Fig. 2.

the effective cavity-magnon interaction and the magnon Kerr nonlinearity under the near resonant conditions. It naturally induces more obvious asymmetry of the microwave transmission in two directions.

To obtain the optimal magnetic field regime for the nonreciprocity transmission, the isolation ratio I as a function of the microwave photon-tunneling rate J and the magnetic field H_z in the non-Hermitian CMS has been intuitively shown in Fig. 7. The isolation ratio I is characterized by a symmetrical distribution with respect to $H_z = 360.7$mT. Especially, in the vicinity of the exceptional point, the light bright area distributed near $H_z = 360.7$mT, where the isolation ratio can be higher than 70 dB. This means the unidirectional nonreciprocal transmission of microwave fields, which can be used to make isolators. In addition, we can observe that, near the exceptional point, strong transmission nonreciprocity can always be achieved in the optimal magnetic field range $H_z \in [359.5 \quad 362]$mT. It means that the bandwidth of optimal detuning regime is seventy megahertz. This regime is achievable for experimental operation to capture robust transmission nonreciprocity in practice.

IV. Conclusion

In summary, we have theoretically provided an approach to realize strong microwave transmission nonreciprocity in a compound three-mode non-Hermitian CMS. It is composed of two gain-loss microwave cavities and one YIG sphere. Our approach is accomplished by regulating the microwave photon-tunneling rate in the non-Hermitian system. We showed that huge asymmetry of the microwave transmissions along two directions can be realized when the cavities and the microwave fields are in resonance or near resonance, by just regulating the microwave photon-tunneling rate. We also presented the influence of the external magnetic field on the microwave transmission along two directions under different microwave photon-tunneling rates. We found that, around the the exceptional point, strong transmission nonreciprocity can be achieved over an optimal magnetic field range. In essence, it is the joint effect of the cavity-magnon near resonant (or resonant) interaction and the effective magnon Kerr nonlinearity in the three-mode non-Hermitian CMS. This study provides a promising route for regulating the microwave nonreciprocity transmission in a three-mode non-Hermitian CMS, and has potential applications in unidirectional transmission.

Acknowledgment

We acknowledge professor Xin-You Lü for his valuable suggestions on our work.

References

[1] F. Marquardt and S. M. Girvin, "Trend: Optomechanics," *Physics*, vol. 2, pp. 40–47, 2009.
[2] M. Aspelmeyer, T. J. Kippenberg, and F. Marquardt, "Cavity optomechanics," *Rev. Mod. Phys.*, vol. 86, no. 4, pp. 1391–1452, 2014.
[3] H. Xiong, L.-G. Si, X.-Y. Lü, X. Yang, and Y. Wu, "Carrier-envelope phase-dependent effect of high-ordersideband generation in ultrafast driven optomechanical system," *Opt. Lett.*, vol. 38, no. 3, pp. 353–355, 2013.
[4] H. Xiong, "Optomechanically induced Benjamin CFeir instability," *Laser Photon. Rev.*, vol. 17, 2023, Art. no. 2200935.
[5] Q. Bin, X.-Y. Lü, F. P. Laussy, F. Nori, and Y. Wu, "N-phonon bundle emission via the stokes process," *Phys. Rev. Lett.*, vol. 124, no. 5, 2020, Art. no. 053601.
[6] M. Wang, P. Meystre, W. Zhang, and Q. He, "Steady-state atom-light entanglement with engineered spin-orbit coupling," *Phys. Rev. A*, vol. 93, no. 4, 2016, Art. no. 042311.
[7] B. Rameshti et al., "Cavity magnonics," *Phys. Rep.*, vol. 979, pp. 1–61, 2022.
[8] Y. P. Wang, G. Q. Zhang, D. Zhang, T. F. Li, C. M. Hu, and J. Q. You, "Bistability of cavity magnon-polaritons," *Phys. Rev. Lett.*, vol. 120, no. 5, 2018, Art. no. 057202.
[9] M. Goryachev, W. G. Farr, D. L. Creedon, Y. Fan, M. Kostylev, and M. E. Tobar, "High-cooperativity cavity QED with magnons at microwave frequencies," *Phys. Rev. Appl.*, vol. 2, no. 5, 2014, Art. no. 054002.
[10] S. Sharma, B. Z. Rameshti, Y. M. Blanter, and G. E. W. Bauer, "Optimal mode matching in cavity optomagnonics," *Phys. Rev. B*, vol. 99, no. 21, 2019, Art. no. 214423.
[11] C. Braggio, G. Carugno, M. Guarise, A. Ortolan, and G. Ruoso, "Optical manipulation of a magnon-photon hybrid system," *Phys. Rev. Lett.*, vol. 118, no. 10, 2017, Art. no. 107205.
[12] X. Zhang, C.-L. Zou, L. Jiang, and H. X. Tang, "Strongly coupled magnons and cavity microwave photons," *Phys. Rev. Lett.*, vol. 113, no. 15, 2014, Art. no. 156401.
[13] J. T. Hou and L. Liu, "Strong coupling between microwave photons and nanomagnet magnons," *Phys. Rev. Lett.*, vol. 123, no. 10, 2019, Art. no. 107702.
[14] Ö. O. Soykal and M. E. Flatté, "Strong field interactions between a nanomagnet and a photonic cavity," *Phys. Rev. Lett.*, vol. 104, no. 7, 2010, Art. no. 077202.
[15] N. Crescini, C. Braggio, G. Carugno, A. Ortolan, and G. Ruoso, "Cavity magnon polariton based precision magnetometry," *Appl. Phys. Lett.*, vol. 117, 2020, Art. no. 144001.
[16] Y. Cao and P. Yan, "Exceptional magnetic sensitivity of PT -symmetric cavity magnon polaritons," *Phys. Rev. B*, vol. 99, no. 21, 2019, Art. no. 214415.
[17] H. Xiong, "Magnonic frequency combs based on the resonantly enhanced magnetostrictive effect," *Fundam. Res.*, vol. 3, pp. 8–14, 2023.
[18] Y. Tabuchi et al., "Coherent coupling between a ferromagnetic magnon and a superconducting qubit," *Science*, vol. 349, no. 6246, pp. 405–408, 2015.
[19] J. Li, S.-Y. Zhu, and G. S. Agarwal, "Squeezed states of magnons and phonons in cavity magnomechanics," *Phys. Rev. A*, vol. 99, no. 2, 2019, Art. no. 021801(R).
[20] X. Zhang, C.-L. Zou, L. Jiang, and H. X. Tang, "Cavity magnomechanics," *Sci. Adv.*, vol. 2, 2016, Art. no. e1501286.
[21] Y.-P. Gao, C. Cao, T.-J. Wang, Y. Zhang, and C. Wang, "Cavity-mediated coupling of phonons and magnons," *Phys. Rev. A*, vol. 96, 2017, Art. no. 023826.
[22] L. Wang et al., "Magnon blockade in a PT-symmetric-like cavity magnomechanical system," *Annalen der Physik*, vol. 532, 2020, Art. no. 2000028.

[23] S. V. Kusminskiy, H. X. Tang, and F. Marquardt, "Coupled spin-light dynamics in cavity optomagnonics," *Phys. Rev. A*, vol. 94, no. 3, 2016, Art. no. 033821.

[24] J. A. Haigh et al., "Magneto-optical coupling in whispering-gallery-mode resonators," *Phys. Rev. A*, vol. 92, no. 6, 2015, Art. no. 063845.

[25] H. Huebl et al., "High cooperativity in coupled microwave resonator ferrimagnetic insulator hybrids," *Phys. Rev. Lett.*, vol. 111, no. 12, 2013, Art. no. 127003.

[26] Y.-P. Wang et al., "Nonreciprocity and unidirectional invisibility in cavity magnonics," *Phys. Rev. Lett.*, vol. 123, no. 12, 2019, Art. no. 127202.

[27] X. Zhang, A. Galda, X. Han, D. Jin, and V. M. Vinokur, "Broadband nonreciprocity enabled by strong coupling of magnons and microwave photons," *Phys. Rev. Appl.*, vol. 13, no. 4, 2020, Art. no. 044039.

[28] C. Kong, H. Xiong, and Y. Wu, "Magnon-induced nonreciprocity based on the magnon Kerr effect," *Phys. Rev. Appl.*, vol. 12, no. 3, 2019, Art. no. 034001.

[29] Y.-j. Xu and J. Song, "Nonreciprocal magnon laser," *Opt. Lett.*, vol. 46, pp. 5276–5279, 2021.

[30] R. El-Ganainy et al., "Non-Hermitian physics and PT symmetry," *Nature Phys.*, vol. 14, pp. 11–19, 2018.

[31] A. Krasnok, N. Nefedkin, and A. Alú, "Parity-time symmetry and exceptional points [electromagnetic perspectives]," *IEEE Antennas Propag. Mag.*, vol. 63, no. 6, pp. 110–121, Dec. 2021.

[32] D. Zhang et al., "Observation of the exceptional point in cavity magnon-polaritons," *Nature Commun.*, vol. 8, 2017, Art. no. 1368.

[33] C. M. Bender and S. Boettcher, "Real spectra in non-Hermitian Hamiltonians having PT symmetry," *Phys. Rev. Lett.*, vol. 80, no. 24, pp. 5243–5246, 1998.

[34] C. M. Bender, "Making sense of non-Hermitian Hamiltonians," *Rep. Prog. Phys.*, vol. 70, no. 6, pp. 947–1018, 2007.

[35] K. G. Makris, R. El-Ganainy, D. N. Christodoulides, and Z. H. Musslimani, "Beam dynamics in PT symmetric optical lattices," *Phys. Rev. Lett.*, vol. 100, no. 10, 2008, Art. no. 103904.

[36] S. Klaiman, U. Günther, and N. Moiseyev, "Visualization of branch points in PT-Symmetric waveguides," *Phys. Rev. Lett.*, vol. 101, no. 8, 2008, Art. no. 080402.

[37] A. Guo et al., "Observation of PT-Symmetry breaking in complex optical potentials," *Phys. Rev. Lett.*, vol. 103, no. 9, 2009, Art. no. 093902.

[38] H. Xu, D.-G. Lai, Y.-B. Qian, B.-P. Hou, A. Miranowicz, and F. Nori, "Optomechanical dynamics in the PT- and broken-PT-symmetric regimes," *Phys. Rev. A*, vol. 104, no. 5, 2021, Art. no. 053518.

[39] B. Peng et al., "Parity Ctime-symmetric whispering-gallery microcavities," *Nature Phys.*, vol. 10, pp. 394–398, 2014.

[40] R. Huang et al., "Exceptional photon blockade: Engineering photon blockade with chiral exceptional points," *Laser Photon. Rev.*, vol. 16, no. 7, 2022, Art. no. 2100430.

[41] H. Jing, Ş. K. Özdemir, X.-Y. Lü, J. Zhang, L. Yang, and F. Nori, "PT-Symmetric phonon laser," *Phys. Rev. Lett.*, vol. 113, no. 5, 2014, Art. no. 053604.

[42] Y. Liu, T. Hao, W. Li, J. Capmany, N. Zhu, and M. Li, "Observation of parity-time symmetry in microwave photonics," *Light: Sci. Appl.*, vol. 7, pp. 1–9, 2018.

[43] S. Bittner et al., "Symmetry and spontaneous symmetry breaking in a microwave billiard," *Phys. Rev. Lett.*, vol. 108, 2021, Art. no. 024101.

[44] J. Schindler, A. Li, M. C. Zheng, F. M. Ellis, and T. Kottos, "Experimental study of active LRC circuits with PT symmetries," *Phys. Rev. A*, vol. 84, no. 4, 2011, Art. no. 040101.

[45] J. N. Bender et al., "Observation of asymmetric transport in structures with active nonlinearities," *Phys. Rev. Lett.*, vol. 110, no. 23, 2013, Art. no. 234101.

[46] X. Zhu, H. Ramezani, C. Shi, J. Zhu, and X. Zhang, "PT-Symmetric acoustics," *Phys. Rev. X*, vol. 4, no. 3, 2014, Art. no. 031042.

[47] R. Fleury, D. Sounas, and A. Alu, "An invisible acoustic sensor based on parity-time symmetry," *Nature Commun.*, vol. 6, 2015, Art. no. 5905.

[48] C. Shi et al., "Accessing the exceptional points of parity-time symmetric acoustics," *Nature Commun.*, vol. 7, 2016, Art. no. 11110.

[49] Y. Li et al., "Antiparity-time symmetry in diffusive systems," *Science*, vol. 364, pp. 170–173, 2019.

[50] C. Dembowski et al., "Experimental observation of the topological structure of exceptional points," *Phys. Rev. Lett.*, vol. 86, no. 5, pp. 787–790, 2001.

[51] X.-W. Xu, L. N. Song, Q. Zheng, Z. H. Wang, and Y. Li, "Optomechanically induced nonreciprocity in a three-mode optomechanical system," *Phys. Rev. A*, vol. 98, no. 6, 2018, Art. no. 063845.

[52] Y. Jiang, S. Maayani, T. Carmon, F. Nori, and H. Jing, "Nonreciprocal phonon laser," *Phys. Rev. Appl.*, vol. 10, no. 6, 2018, Art. no. 064037.

[53] B. Peng et al., "Loss-induced suppression and revival of lasing," *Science*, vol. 346, no. 6207, pp. 328–332, 2014.

[54] L. Chang et al., "Parity ctime symmetry and variable optical isolation in active cpassive-coupled microresonators," *Nat. Photon.*, vol. 8, pp. 524–529, 2014.

[55] L. Feng, Z. J. Wong, R.-M. Ma, Y. Wang, and X. Zhang, "Single-mode laser by parity-time symmetry breaking," *Science*, vol. 346, no. 6212, pp. 972–975, 2014.

[56] H. Hodaei, M.-A. Miri, M. Heinrich, D. N. Christodoulides, and M. Khajavikhan, "Parity-time csymmetric microring lasers," *Science*, vol. 346, no. 6212, pp. 975–978, 2014.

[57] J. Li, J. Li, Q. Xiao, and Y. Wu, "Giant enhancement of optical high-ordersideband generation and their control in a dimer of two cavities with gain and loss," *Phys. Rev. A*, vol. 93, 2016, Art. no. 063814.

[58] X.-Y. Lü, H. Jing, J.-Y. Ma, and Y. Wu, "PT-symmetry-breaking chaos in optomechanics," *Phys. Rev. Lett.*, vol. 114, no. 25, 2015, Art. no. 253601.

[59] Z. Zhang, Y.-P. Wang, and X. Wang, "PT -symmetry-breaking-enhanced cavity optomechanical magnetometry," *Phys. Rev. A*, vol. 102, no. 2, 2020, Art. no. 023512.

[60] B. Wang, X. Jia, X.-H. Lu, and H. Xiong, "PT-symmetric magnon laser in cavity optomagnonics," *Phys. Rev. A*, vol. 105, 2022, Art. no. 053705.

[61] G.-Q. Zhang and J. Q. You, "Higher-order exceptional point in a cavity magnonics system," *Phys. Rev. B*, vol. 99, 2019, Art. no. 054404.

[62] L.-Y. He, "Parity-time-symmetry-enhanced sideband generation in an optomechanical system," *Phys. Rev. A*, vol. 99, no. 3, 2019, Art. no. 033843.

[63] Y.-P. Wang, G.-Q. Zhang, D. Zhang, T.-F. Li, C.-M. Hu, and J.-Q. You, "Bistability of cavity magnon polaritons," *Phys. Rev. Lett.*, vol. 120, no. 5, 2018, Art. no. 057202.

[64] Q. Shao and K. L. Wang, "Heat-assisted microwave amplifier," *Nature Nanotechnol.*, vol. 14, pp. 9–11, 2019.

[65] H. Suhl, "The ferromagnetic microwave amplifier," *Phys. Today*, vol. 11, no. 9, pp. 28–30, 1958.

[66] A. Alberucci and G. Assanto, "All-optical isolation by directional coupling," *Opt. Lett.*, vol. 33, no. 15, pp. 1641–1643, 2008.

[67] S. Guddala et al., "All-optical nonreciprocity due to valley polarization pumping in transition metal dichalcogenides," *Nature Commun.*, vol. 12, 2021, Art. no. 3746.